

Gravitational-wave asteroseismology with f -modes from neutron star binaries at the merger phase

Harry Ho-Yin Ng,^{*} Patrick Chi-Kit Cheong,[†] Lap-Ming Lin,[‡] and Tjonnie Guang Feng Li[§]
Department of Physics, The Chinese University of Hong Kong, Shatin, N.T., Hong Kong
(Dated: 15 December 2020)

Gravitational-wave signals from coalescing binary neutron stars can yield important information about the properties of nuclear-matter equation of state from the early part of the signal through tidal effects to the properties and oscillation frequencies of the merger product. In this work, we investigate a direct link between the properties of isolated neutron stars and their merger, by comparing the frequency of the fundamental oscillation mode (f -mode) of neutron stars with the gravitational-wave frequency associated with the merger of two neutron stars. In particular, we calculate the quadrupolar ($l = 2$) f -mode oscillation (f_{2f}) of non-rotating and rotating neutron stars using a nonlinear hydrodynamics code in the conformally-flat approximation and obtain the gravitational-wave frequency associated with the peak amplitude (f_{\max}) of binary-neutron stars from a set of publicly available simulations. We find that f_{\max} and f_{2f} differ by about 1%, on average, across forty-five equal-mass systems with different total mass and equations of state. Interestingly, assuming that the gravitational-wave frequency is still approximately equal to twice the orbital frequency Ω near the merger, the result indicates that the condition for tidal resonance $|m|\Omega = f_{2f}$ is satisfied to high accuracy near the merger, where $m = 2$ is the azimuthal quantum number. While it has been suggested that the resonance condition could be satisfied near the merger phase, this is the first time that the accuracy of the resonance condition is quantified. Moreover, the well established universal relation between f_{\max} and the tidal deformability of equal-mass binary systems can now be explained by a similar relation between f_{2f} and the tidal deformability of isolated neutron stars, which has been demonstrated to be associated with the nearly incompressible properties of neutron stars. For unequal-mass binaries, f_{\max} is generally smaller than the f -mode frequencies of the two stars, and the deviation increases as the mass ratio decreases from unity for the limited systems that we have surveyed. Therefore, our findings suggest that it is possible to relate the gravitational-wave signal at the merger of a binary neutron star system directly to the fundamental oscillation modes and the mass ratio. This work potentially brings gravitational-wave asteroseismology to the late-inspiral and merger phases of binary neutron stars, filling the gap between the early inspiral and post-merger signals.

I. INTRODUCTION

The observation of gravitational waves (GWs) from binary neutron star (BNS) systems will be an important channel to probe the uncertain properties of the supra-nuclear equation of state (EOS) and may even provide evidence for the existence of deconfined quark matter and phase transitions inside neutron stars (NSs) [1–4].

Studies have shown that different physical effects imprint various signatures in the GW signal during the inspiral and post-merger phases of a BNS system [5, 6]. The inspiral phase depends on the EOS through the tidal deformability λ_l of an NS, which characterizes the multipole moments (order l) of the deformation induced by the tidal field of the companion [7, 8]. The tidal deformability is known to be sensitive to the EOS of NS matter [9, 10]. The analysis of the first GW observation of a BNS (GW170817) has already put limits on this parameter and provided constraints on various EOSs [10–12].

The internal oscillation modes of NSs can be excited by

the tidal field during the inspiral. The quadrupolar $l = 2$ fundamental fluid mode (2f -mode) is expected to have the strongest tidal coupling because it vibrates like standing waves on the surface of the NS and the amplitude extends towards the surface [13, 14]. The coupling between the excited 2f -modes and tidal fields has been found to lead to dynamical tidal effects, which becomes dominant when the tidal forcing frequency approaches the 2f -mode frequency [15]. This effect results in frequency-dependent tidal deformability (or tidal Love number k_l) and an extra phase-shift in the emitted GW beyond the static tide limit [15, 16]. The inclusion of the dynamical tidal contribution in the analysis of GW170817 has placed constraints on the 2f -mode frequency [6].

The 2f -mode of NSs is also interesting in its own right as its frequency, in general, depends sensitively on the EOS and the spin of the star [17, 18]. For example, the post-merger GW signals due to the 2f -mode oscillations of the hypermassive NS formed after the merger can also provide us an important channel to study the hot EOS and properties of the merger remnant [5, 19–22].

In this paper, we add a twist to the story by considering, instead of the inspiral and post-merger phases, whether the GW signals *at* the merger can be used to probe the 2f -modes of the two initial NSs. The merger signal has an obvious advantage in that the GW ampli-

^{*} hoyin.ng@ligo.org

[†] chi-kit.cheong@ligo.org

[‡] lmlin@phy.cuhk.edu.hk

[§] tgfli@cuhk.edu.hk

tude is the largest. While current detectors are not yet sensitive enough in the high frequency range (~ 1000 – 2000 Hz) to detect the merger signals directly, it might not be too far away for current detectors such as Advanced LIGO [23], Advanced Virgo [24], KAGRA [25] and future detectors such as Einstein Telescope [26]. Depending on the EOS models, the GW frequency at the merger is in general also somewhat lower than those signals associated with the oscillations of the post-merger hypermassive NS [20, 21], making it more promising to be detected.

The merger phase is characterized by a maximum in the GW amplitude which in turn signals the end of the inspiral phase. The frequency at the maximum amplitude f_{\max} has been well studied in BNS simulations [9, 21, 27]. It is also found that there exists a strong correlation between f_{\max} and the tidal deformability (expressed by the tidal coupling constant κ_2^T).

We consider the numerical data for different BNS systems published in [21, 28, 29]. Surprisingly, we find that the values of f_{\max} for equal-mass binaries agree very well to those of the 2f -mode frequencies f_{2f} of the two non-rotating and rotating initial NSs that we computed using a hydrodynamics code [30]. In particular, the average relative difference between f_{\max} and f_{2f} is about 1% level across the EOS models and mass range ($1.2 - 1.4M_\odot$) that we have considered. The close relation between f_{\max} and f_{2f} leads us to propose that the universal relation (UR) connecting f_{\max} and κ_2^T for BNS systems [21, 31, 32], originates from the UR between the 2f -mode frequencies and the tidal deformability for isolated NSs as found in [33]. For unequal-mass binaries, the correlation between the two frequencies becomes weaker and the largest relative difference in our data set is about -35.5% . With the limited data set that we have for unequal-mass binaries, we see hints that the difference between the two frequencies increases as the mass ratio decreases from unity. Our study, therefore, suggests that one can obtain information about the 2f -mode frequency and mass ratio q of a BNS system using the GW peak frequency f_{\max} at the merger phase. Unless otherwise stated, physical quantities are represented in dimensionless units $c = G = M_\odot = 1$.

II. NUMERICAL SETUP

A. Fundamental oscillation mode of rotating neutron stars

We follow the approach of Ref. [18] to determine the frequency of 2f -mode frequency of an isolated NS by suitably perturbing and following the evolution of the star by a non-linear hydrodynamics code. We employ an open-sourced code XNS [34, 35], supplemented with realistic EOSs with piecewise polytropic approximation, to generate axisymmetric uniformly rotating NSs to serve as initial data for our simulations. We consider 3 sequences

of fixed angular velocity a , namely a non-rotating sequence (U0) and two rotating sequences with frequencies 418 Hz (U1) and 673 Hz (U2). For each sequence, we consider NSs with different gravitational mass ranging from $M_g = 1.20$ to $1.60 M_\odot$, which are modeled by 6 different realistic cold EOSs: APR4 [36], SLY [37], ENG [38], ALF2 [39], GNH3 [40] and H4 [41]. These EOSs all satisfy the current observational lower bound on the maximum mass [42]. To save computational time and minimize interpolation errors, we use piecewise polytropic approximations each with 4 pieces instead of tabulated EOSs, which have been shown to reproduce sufficiently accurate representations [31]. In particular, inside the range of $\rho_{i-1} \leq \rho < \rho_i$, with $i = 1, 2, 3, 4$,

$$p = K_i \rho^{\Gamma_i}, \quad (1)$$

$$\epsilon(\rho) = (1 + A_i) \rho + \frac{K_i}{\Gamma_i - 1} \rho^{\Gamma_i}, \quad (2)$$

$$A_i = \frac{\epsilon(\rho_{i-1})}{\rho_{i-1}} - 1 - \frac{K_i}{\Gamma_i - 1} \rho_{i-1}^{\Gamma_i - 1}, \quad (3)$$

where ρ is the rest-mass density, ϵ is the energy density, p is the pressure, and the constants ρ_i are the cut-off rest-mass density to define the boundaries separating the polytropic models. The variables ρ , ϵ , and p are assumed to be continuous at the boundaries. The parameters Γ_i and K_i are the adiabatic indices and polytropic constants for the different regions.

We use a new relativistic hydrodynamics code `Gmunu` [30] for the evolution of the initial NS. `Gmunu` uses a multi-grid method to solve the Einstein equations in the conformally flat condition (CFC) approximation, which has been shown to solve the elliptic-type metric equations resulting in the CFC approximation efficiently. `Gmunu` also includes standard high-resolution shock-capturing (HRSC) schemes to solve the hydrodynamics equations, and the Harten-Lax-van Leer-Einfeldt (HLL) Riemann solver [43] with the TVD reconstruction scheme [44]. The time update uses a 3rd order Runge-Kutta method. While the code is not fully general relativistic, the CFC approximation has been demonstrated to be a good approximation to model various astrophysical problems [18, 45–48].

We perform axisymmetric simulations using spherical coordinates (r, θ) with an equidistantly spaced grid resolution $n_r \times n_\theta = 320 \times 32$. In our simulations, the interior of a typical NS model is resolved by about 120 to 200 grid points along the radial direction. The outside region of the star is covered by an artificial atmosphere with a density $\rho_{atm} \sim 10^{-7} \rho_c$, where ρ_c is the central density of the star. The metric is solved at every 50 hydrodynamic steps and we extrapolate the metric in between. We evolve the initial profiles by `Gmunu` by adding the following θ -component velocity perturbation to excite the $l = 2$, $m_l = 0$ axisymmetric 2f -mode of rotating NSs [18]:

$$v_\theta = A \sin\left(\pi \frac{r}{r_s(\theta)}\right) (3 \cos^2 \theta - 1), \quad (4)$$

where $r_s(\theta)$ is the coordinate radius of the stellar surface and the perturbation amplitude is chosen to be $A = 0.01$. While this perturbation function is not an exact mode eigenfunction, it is chosen to mimic the angular dependence of the axisymmetric 2f -mode so that this mode can be excited and dominate other modes during the evolution of a slowly rotating star. For rapidly rotating stars, other oscillation modes can also be excited or even be stronger than the 2f -mode that we focus on [18]. We note that non-axisymmetric modes cannot be studied in our axisymmetric simulations.

The evolution time for each model is around 60 – 80 ms (~ 5 -20 spinning cycles) which we have found to be sufficient for extracting the 2f -mode. The mode is identified and its frequency is obtained by performing a Fourier transform of the non-radial velocity component v^θ at $n_r = 80$, $\theta = \pi/4$ which is ensured to be inside the star (see [33] for more details).

B. Tidal coupling constant κ_2^T

The rescaled tidal coupling parameter κ_2^T of a BNS system is defined from the $l = 2$ dimensionless tidal Love numbers k_2^A and k_2^B of two NSs A and B of the system when they are at infinite separation [49], namely

$$\kappa_2^T \equiv 2 \left[q \left(\frac{X_A}{C_A} \right)^5 k_2^A + \frac{1}{q} \left(\frac{X_B}{C_B} \right)^5 k_2^B \right], \quad (5)$$

$$q \equiv \frac{M_B}{M_A} \leq 1, \quad (6)$$

$$X_{A,B} \equiv \frac{M_{A,B}}{M_A + M_B}, \quad (7)$$

$$C_{A,B} \equiv M_{A,B}/R_{A,B}, \quad (8)$$

where q is the mass ratio, $C_{A,B}$, $M_{A,B}$ and $R_{A,B}$ are the compactness, gravitational mass, and radius of A and B when they are at infinite separation. For equal-mass binaries,

$$k_2^A = k_2^B = k_2, \quad (9)$$

and hence Eq. (5) becomes

$$\kappa_2^T \equiv \frac{1}{8} k_2 \left(\frac{R}{M} \right)^5 = \frac{3}{16} \lambda_2. \quad (10)$$

The quadrupolar tidal deformability λ_2 is given by

$$\lambda_2 \equiv \frac{2}{3} k_2 \left(\frac{R}{M} \right)^5, \quad (11)$$

where $M = M_A = M_B$ and $R = R_A = R_B$. Unless otherwise noted, we put a bar on top of a variable to denote its average value, such as the average mass \bar{M} , for unequal-mass binaries. We will also use Eq. (10) to define a rescaled tidal coupling constant for an isolated NS.

III. RESULTS

A. Comparing the frequencies of the fundamental oscillation modes to the peak GW amplitude

In this section, we compare the 2f -mode frequency (f_{2f}) of the NSs when they are at infinite separation (see Sec. II) to the frequency of the peak GW amplitude from BNS simulations (f_{\max}) reported in the literature [21, 28, 29, 33]. In particular, Ref. [21] contains 56 BNS merger simulations assuming initially quasi-equilibrium irrotational initial data (52 equal-mass binaries, 4 unequal-mass binaries). The simulations span a range of average masses $\bar{M} = 1.20 - 1.50 M_\odot$ and 6 cold EOSs (i.e. APR4, SLY, ALF2, GNH3, H4, LS220 [50]) with an additional thermal contribution. During the whole inspiral phase, binaries orbit at least 4 orbits or more before the moment of merger (defined as the time when the GW amplitude attained maximum), and till the postmerger phase where a hypermassive NS survived for ≈ 25 ms. The instantaneous frequency of the GW during the inspiral is computed from the phase ϕ of the waveform, which is related to the dominant $l = m = 2$ mode of the multipolar expansion of the Weyl curvature scalar Ψ_4 [51]. The values of the GW frequency at the time of merger f_{\max} are shown in the Tab. II of Ref. [21].

Moreover, we use 12 data points of the merger GW frequency f_{mrg} for unequal-mass, non-spinning initial data presented in Tab. I of Ref. [28] and Tab. V of Ref. [29] (using R2 data). The definition of f_{mrg} is the same as f_{\max} for unequal-mass binaries. The binaries have average masses $\bar{M} = 1.25 - 1.375 M_\odot$, mass ratio $q = 0.571, 0.667, 0.8, \text{ and } 0.9$ (two for $q = 0.9$, five for $q = 0.8$, six for $q = 0.667$, and two for $q = 0.571$), which are modeled by various EOSs including SLY, ALF2, GNH3, and H4.

Fig. 1 shows f_{2f} against the mass of isolated NS (solid lines) and f_{\max} against the average mass of BNS systems (star-shaped markers connected by dashed lines), for various EOSs (colors). Note that the EOSs for BNS simulations include an additional thermal contribution to account for the shock heating, while in our simulations of isolated NSs, we use the same set of cold EOSs but without the thermal contribution.

The 2f -mode data in Fig. 1 consist of three solid lines per EOS (i.e. per color) that correspond to the three spin-frequency sequences (U0, U1, and U2). Therefore, the band for each EOS represents the range of the values of f_{2f} for the range of spin frequency from 0 to 673 Hz. For SLY, APR4, and ALF2 EOSs, we find that f_{2f} increases with the spin frequency so that the non-rotating sequence U0 is given by the bottom solid line in the color bands, while the rotating sequences U1 and U2 are represented by the middle and top solid lines. On the other hand, the U2 sequence of the GNH3 model has the lowest f_{2f} values and is represented by the bottom line in the green color band. Finally, the value of f_{2f} for H4 model is somewhat insensitive to the rotation for the range of spin frequency we used so that the band is barely vis-

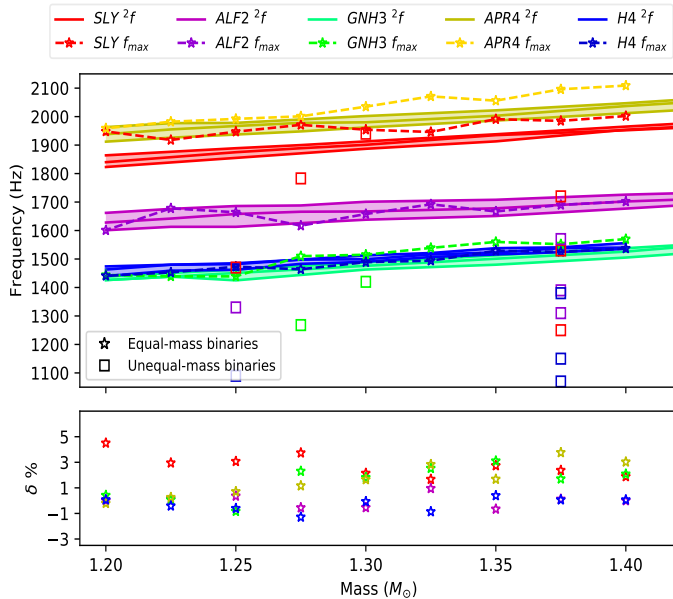


FIG. 1. *Upper panel:* The 2f -mode frequencies f_{2f} (solid line) for three spin sequences (U0, U1, and U2) are plotted against the gravitational mass M of the isolated stars. Moreover, the merger gravitational wave peak frequencies f_{\max} of equal-mass binaries (star-shaped markers connected by dashed lines) and unequal-mass binaries (square-shaped markers) are plotted against the average mass \bar{M} . Different colors represent the results from the different EOSs (SLY in red, ALF2 in purple, GNH3 in green, APR4 in yellow, and H4 in blue). *Lower panel:* Relative difference % between f_{\max} for the equal-mass binaries and the closest value of f_{2f} among the 3 spin sequences with the same EOS and mass.

ible. The strong dependence of f_{2f} on the EOS, spin frequency, and the mass of NS are clearly reflected by the different range and width of the color bands.

Let us begin by focusing on comparison between f_{\max} and f_{2f} for equal-mass binaries (star-shaped markers). The lower panel in Fig. 1 shows the relative difference δ between the value of f_{\max} and the closest value of f_{2f} of the band for a given EOS and mass M . The average δ for APR4, SLY, ALF2, GNH3, and H4 are +1.65%, +2.79%, -0.22%, +1.47%, and -0.29% respectively. We note that, in general, f_{\max} has a higher value than f_{2f} . Moreover, we observe that there is a better match between f_{\max} and f_{2f} for stiffer EOSs. The exception is for the softer ALF2, which has the lowest values of δ . This exception can be explained by the definition of δ , which is the relative difference between f_{\max} and the nearest value for f_{2f} among the three rotation profiles for a given mass. The relatively large spread of the f_{2f} values for ALF2 means that it is more likely to produce a lower value of δ . For the softest EOSs, SLY and APR4, the difference between f_{\max} and f_{2f} are generally larger than those of the stiffer models. This may be due to the limited spin values that we have used. Indeed, for soft EOSs, higher spin values typically induce higher f_{2f} , so that the rel-

ative difference δ could further decrease by considering faster spinning models. Nevertheless, the data in Fig. 1 are sufficient to demonstrate the closeness between f_{2f} and f_{\max} .

Let us turn to the comparison between f_{\max} and f_{2f} for unequal-mass binaries (the relative differences are not shown in the lower panel of Fig. 1 as they, in general, are significantly larger than those of equal-mass binaries). In particular, the average δ across data with different mass ratios for SLY, ALF2, GNH3, H4 EOSs are -16.0% (6 data points), -15.2% (4 data points), -7.6% (2 data points) and -22.3% (4 data points) respectively. We observe that the average δ becomes more negative as the mass ratio q (less than or equal to unity, as defined in Eq. (6)) decreases for all EOSs. In general, the value of f_{\max} is lower for unequal-mass binaries than for equal-mass binaries. In fact, f_{\max} for unequal-mass binaries is even lower than f_{2f} of the lightest NS. For example, for the case of GNH3 with $q = 0.9$ and $\bar{M} = 1.3M_{\odot}$ we have $f_{\max} = 1420$ Hz and the 2f -mode frequency of the less (more) massive non-rotating isolated NS with $M = 1.232$ ($M = 1.368$) is 1455 Hz (1577 Hz). We observe that the relative difference δ decreases rapidly as $q \rightarrow 1$. In particular, the average relative differences are -6.2% and -24.2% for $q \geq 0.8$ and $q < 0.8$ respectively.

The similarity between f_{2f} and f_{\max} for equal-mass binaries leads us to conjecture that there may be strong coupling between the 2f -mode and tidal fields as the tidal forcing frequency near the merger approaches the 2f -mode frequency. We will discuss the physical aspects of our results in more detail in Sec. IV. However, we first use the similarity between f_{2f} and f_{\max} to provide a plausible origin of the $Mf_{\max} - \kappa_2^T$ UR proposed in recent literature [9, 21, 27].

B. Universal relations

Recent studies have empirically established that f_{\max} for equal-mass binaries has a strong correlation with the tidal coupling constant κ_2^T through an approximately EOS-insensitive UR [9, 21, 27, 32]. Interestingly, it has also been found that there exists an UR connecting the 2f -mode frequency and the tidal deformability of nonrotating cold NSs [33]. In this section, by using the finding that $f_{\max} \approx f_{2f}$ for equal-mass binaries from Sec. III A, we provide a plausible origin for the $Mf_{\max} - \kappa_2^T$ relation.

There are several slightly different empirical fitting curves for the $Mf_{\max} - \kappa_2^T$ relation obtained by different groups [9, 21, 27]. In this work, we use the fit given by Eqs. (15) and (17) of Ref. [21] and plot it as a black dashed line in Fig. 2. For equal-mass binaries, the average deviation between the values of f_{\max} and those predicted by the fit is only about +1.3% [21]. Similarly, after replacing λ_2 by κ_2^T as explained in Sec. II B, the $Mf_{2f} - \lambda_2$ fitting curve for nonrotating NSs (cf. Eq. (3.5) of Ref. [33]) is plotted as a yellow dotted line in the same figure for comparison. This 2f -mode-Love relation

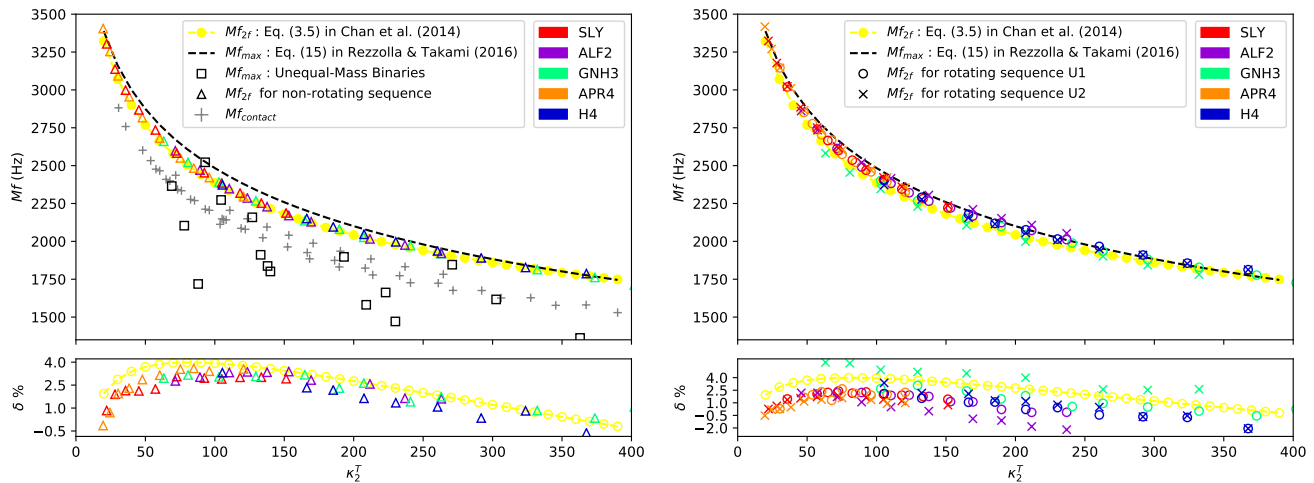


FIG. 2. *Upper panel*: The UR (black dashed fit) of the mass-weighted merger GW peak frequencies Mf_{\max} plotted against the tidal coupling constant κ_2^T obtained from [21] is shown in both of the plots above. The UR (yellow dotted fit) of the mass-weighted 2f -mode frequencies of non-rotating NSs plotted against the tidal coupling constant κ_2^T is also shown in the plots above. The mass-weighted 2f -mode frequencies Mf_{2f} for the three spin sequences from U0 to U2 (U0 : Δ in the left figure of Fig. 2, U1: \circ and U2: \times in the right figure of Fig. 2) are plotted against the tidal coupling constant κ_2^T . Different colors represent the results of Mf_{2f} from different EOSs. The mass-weighted $\bar{M}f_{\max}$ of unequal-mass binaries for different EOSs (black square-shaped markers) obtained from [21, 28, 29] and mass-weighted estimated contact frequency of BNS Mf_{contact} for different EOSs (grey plus-shaped markers) defined in [52] are also included. *Lower panel*: Relative differences between the values of mass-weighted 2f -mode frequency Mf_{2f} and the black dashed fit with a given tidal coupling constant κ_2^T .

is insensitive to EOS models to about 1.0% level [33]. It is noted that the black dashed fit is above the yellow fit as the values of f_{\max} are slightly higher than those of f_{2f} . The relative differences between the two fits, taking the black dashed fit as a reference, are plotted in the lower panels of Fig. 2. While the two URs were discovered independently for different systems (isolated NSs and BNS systems), it is interesting to see that the two fits agree to high accuracy, especially in the small κ_2^T region. The average deviation between the two fits is about +2.3% across the range of κ_2^T considered in Fig. 2.

As a consistency check, we also plot the f_{2f} data for our non-rotating sequence U0 in the left panel of Fig. 2 (Δ), which are obtained numerically from hydrodynamics evolutions under the CFC approximation. We can see that our data agree with the yellow dotted line, which is obtained from a perturbative quasi-normal mode analysis [33]. Indeed, the average relative differences (δ) is about +2.17% (similar to the difference between the two fitting curves) and is insensitive to the EOS.

Moreover, one might argue that the values of f_{\max} and f_{2f} could indeed be comparable from the perspective of dimensional analysis. In Fig. 2, we also plot the mass-weighted contact frequencies (grey pluses) Mf_{contact} against κ_2^T for comparison. The contact frequency $f_{\text{contact}} = \mathcal{C}^{3/2}/(2\pi M)$ defined in [52], where \mathcal{C} is the compactness, gives a characteristic GW frequency at the merger. While the trend of f_{contact} is similar to the black dashed fit, the data are significantly below the fit. This observation makes it difficult to explain the closeness between the yellow and black fits simply by a

dimensional argument.

The black dashed fit is obtained by fitting 56 BNS simulation data [21] which includes only 4 unequal-mass systems. The black dashed fit is thus dominated by equal-mass BNS data. In Fig. 2, we also plot the values of $\bar{M}f_{\max}$ for unequal-mass binaries presented in [28, 29]. As already noted in [21], the correlation between f_{\max} and κ_2^T becomes weaker for unequal-mass binaries. The deviations (not shown in the lower panel of Fig. 2) between the data and the black dashed fit are significantly larger for smaller mass ratio q . A lower mass ratio q induces a larger deviation from the black dashed line. Specifically, the average δ are +8.93% and +25.0% for $q \geq 0.8$ and $q < 0.8$, respectively. The issue was first stated in Ref. [21], which discussed the “breaking” of the UR for small and possibly unrealistic mass ratio. We explain the “breaking” of the $Mf_{\max} - \kappa_2^T$ relation by the increase of the deviation between f_{\max} and f_{2f} with the decrease of the mass ratio q . With more unequal-mass BNS data available in the future, this could potentially have some observational implications.

Let us now consider the effects of NS rotation. In the right panel of Fig. 2, we plot the 2f -mode data for the spinning sequences U1 (\circ) and U2 (\times) in addition to the two fits. The relative differences between the data and the black dashed fit are shown in the lower panel of Fig. 2. The average δ for U1 and U2 are +1.27% and +1.17%, respectively, which are smaller than the difference (+2.17%) between the two fits. The results show that the effects of NS spin, in general, can help to shift the $Mf_{2f} - \kappa_2^T$ relation toward the black dashed fit be-

cause the values of f_{2f} in general increase with the spin frequency for our chosen EOSs. One exception is the GNH3 model where the deviations for U1 (green circles) are within +2.0%, while those for U2 (green crosses) can be as large as +5.0%. This is due to the fact that the values of f_{2f} of the U2 sequence are smaller than those of the U1 sequence for this EOS as noted above. For softer EOSs such as SLY and APR4, which are commonly employed in the study of NSs, the U2 data have the least deviations from the black dashed fit.

In summary, we find that the $Mf_{\max} - \kappa_2^T$ UR for equal-mass binaries [21] can be explained by the $Mf_{2f} - \kappa_2^T$ for cold isolated NSs [33]. Our conclusion is further strengthened by considering the effects of NS spin on the 2f -mode frequency. It is surprising that the two URs can match so well, even though they were originally discovered for quite different systems (isolated vs binary NS systems). This naturally leads one to ask whether there might be a physical reason for $f_{\max} \approx f_{2f}$ which we will try to address in the next section. Before ending this section, we also remark that the $Mf_{2f} - \kappa_2^T$ UR for isolated NSs can be explained by the nearly incompressible properties of NSs [33]. The $Mf_{\max} - \kappa_2^T$ relation for BNS systems can now be explained similarly.

IV. CONCLUDING REMARKS

In this work, we have investigated the 2f -mode frequencies of isolated NS with 6 different cold EOSs, 3 sequences of nonrotating and uniformly rotating models in the gravitational-mass range $M = 1.20 - 1.40M_{\odot}$. Interestingly, we found a strong correlation between the 2f -mode frequencies f_{2f} of isolated NSs and the instantaneous GW peak frequency f_{\max} of BNS systems at the merger phase. We can summarize the main observations as follows:

- (i) For equal-mass binaries, the 2f -mode frequencies of the two initial NSs agree very well to the GW peak frequency when the two stars merge. The average relative difference between the two frequencies is about 1% across 45 equal-mass systems we have considered.
- (ii) For unequal-mass binaries, these two frequencies deviate significantly. In particular, the difference between f_{2f} and f_{\max} increases as the mass ratio q decreases from unity. For the limited number of unequal-mass BNS data publicly available to us, we found that the average relative differences between the two frequencies are about 6% and 24% for $q \geq 0.8$ and $q < 0.8$, respectively.
- (iii) As a direct consequence of $f_{\max} \approx f_{2f}$, the $Mf_{\max} - \kappa_2^T$ UR for equal-mass binaries [9, 21, 27] can now be explained by the $Mf_{2f} - \kappa_2^T$ UR discovered for isolated non-rotating NSs, which has been

demonstrated to be associated to the nearly incompressible properties of NSs [33]. We also found evidence that rotation can help to improve the agreement between the two URs.

- (iv) The breaking of the $Mf_{\max} - \kappa_2^T$ UR for unequal-mass binaries is a consequence of (ii).

For equal-mass binaries, the observation $f_{\max} \approx f_{2f}$ is very interesting and unexpected. While we cannot rule out the possibility that this result is only a coincidence due to the limited number of BNS data sets that we have surveyed [21, 28, 29], it is still instructive to ask whether there may be an underlying physical mechanism that is responsible for the observation. As mentioned in Sec. I, the quadrupolar 2f -mode has the strongest tidal coupling and can be excited by the tidal fields during the inspiral phase of a BNS system. The coupling between the excited 2f -mode and tidal fields can lead to complicated dynamical tidal effects [15, 16] as the tidal forcing frequency approaches the 2f -mode frequency. In particular, it is well established that the condition for the oscillation mode to be driven resonantly is given by $|m|\Omega = 2\pi f_{2f}$, where m is the azimuthal quantum number and Ω is the orbital angular frequency (e.g., [15]).

For circular binaries, the dominant gravitational-wave frequency f^{GW} during the inspiral is twice the orbital frequency, $f^{GW} = 2\Omega/2\pi$, although higher harmonics with much smaller amplitudes can also exist. Since the BNS data that we have used in this study are generated from quasi-equilibrium irrotational initial data [21, 28, 29], it is expected that $f^{GW} = 2\Omega/2\pi$ is satisfied to high accuracy as these binaries maintain quasi-circular orbits during most of the inspiral phase. However, it is unclear whether this condition still holds in the highly nonlinear dynamical merger phase. Assuming that f^{GW} does not deviate from $2\Omega/2\pi$ significantly, the observation $f_{\max} \approx f_{2f}$ for equal-mass binaries implies that the resonance condition $|m|\Omega/2\pi \approx f_{\max} \approx f_{2f}$ is satisfied to high accuracy at the merger phase with $|m| = 2$. While this observation alone does not necessarily mean that the f -modes of the stars were driven resonantly in the simulations, the f -modes should nevertheless be excited as the tidal driving frequency approaches resonance. The resulting dynamical tidal effects on the emitted GW signals have been well studied [15, 16, 53]. While it has been suggested that the resonance condition could be satisfied near the merger phase, this is the first time that the accuracy of the resonance condition is quantified. Furthermore, one open question is whether the f -modes could grow to large enough amplitudes to affect the orbital dynamics significantly during the last few orbits.

Motivated by the observation that $f_{\max} \approx f_{2f}$, and hence the resonance condition is satisfied to high accuracy at the merger phase across the equal-mass binaries that we have surveyed, we conjecture that the f -modes can grow to large amplitudes and lead to strong tidal coupling in the highly nonlinear regime near the merger. During the last few orbits, the strong tidal coupling draws

the orbital energy to the mode oscillations. When the tidal driving frequency approaches resonance, the energy loss makes the orbit shrink much faster leading to the rapid growth of Ω . The two NSs merge shortly after the resonance condition is satisfied. This explains why $f_{\max} \approx f_{2f}$, and in particular it is slightly larger than f_{2f} , to high accuracy at the moment of merger for all the equal-mass binaries that we have surveyed.

In contrast to the situations of spinning [54, 55] and eccentric binaries [56, 57], where the tidal f -mode resonance has been well studied, it is generally not expected that the f -modes in non-spinning circular binaries can be resonantly excited due to their high frequencies [54, 58]. It should also be noted that the resonances of other low-frequency modes, such as the g -modes and r -modes, have also been studied [54, 58–60]. Our conjecture about the properties of BNS systems in the highly nonlinear merger phase does not necessarily contradict the general expectation based on the linear mode analysis in Newtonian and post-Newtonian approximations. Most importantly, our conjecture should be falsifiable by existing BNS simulation data. By following the fluid motions of the stars in a BNS simulation, one should in principle be able to monitor the growth of the f -mode oscillations (if exist). We notice that such an investigation of the f -mode oscillations has been done for eccentric BNS simulations [61]. Being able to see rapid growth of the f -mode oscillations in the last few orbits near the merger could provide support to our conjecture. On the other hand, the conjecture can be disproved directly if there is no evidence of the f -mode oscillations in the equal-mass BNS simulations that we have surveyed.

For unequal-mass binary cases, we have observed that the values of f_{\max} and f_{2f} differ from each other significantly for the limited number of data that we have studied, and the difference increases as the mass ratio decreases. In addition, f_{\max} is smaller than both values of f_{2f} for the two stars. A possible reason is that the exact moment of merger could not be simply defined as the time of GW signal at maximum amplitude due to the asymmetry of the system, because the smaller mass companion may be tidally disrupted by the more massive companion before the merger. With the disruption of the smaller mass companion, the tidal couplings and excitations of the f -modes become less significant comparing to equal-mass binaries. BNS systems with smaller mass ratio may also result in an earlier disruption of the smaller mass companion, and hence lead to a larger difference between f_{\max} and f_{2f} . Nevertheless, more simulation results are needed to

provide a detailed investigation of this issue.

Advanced LIGO, Advanced Virgo, KAGRA and third-generation GW detectors such as Einstein Telescope will be able to cover the sensitivity band with 1000 – 3000 Hz, making it possible to detect f_{\max} which has the largest amplitude, from the GW signals of BNS systems in the future. Our observation that $f_{\max} \approx f_{2f}$ for equal-mass binaries can be used to yield important information about BNS systems and provide constraints on EOSs. For instance, assuming that the mass ratio ($q \geq 0.9$) of a nearly equal-mass binary can be inferred accurately during the inspiral phase and f_{\max} can also be detected at the merge phase of the same system, then the f -mode frequencies of the stars can be inferred directly. As the f -mode frequency depends sensitively on the EOS, this can help to put constraints on the EOS models. Using the $Mf_{2f} - \kappa_2^T$ UR of [33], one can also infer the tidal deformability from the merger signal and provide a consistency check for the same physical quantity that may be inferred from the GW signals observed in the inspiral phase. On the other hand, one can also turn the argument around and use the tidal deformability inferred in the inspiral phase to constrain the f -mode frequency [6] and compare with f_{\max} . The difference between the two frequencies could provide a way to constrain the mass ratio from the merger signals. However, more unequal-mass BNS simulation data are needed to study how the frequency difference δf varies with the mass ratio and EOS models.

While the GW signals in the post-merger phase are strongly associated with the normal mode oscillations of the hypermassive star formed in the merger [19, 20, 22], it is surprising that the GW frequency at the moment of merger can be correlated so well to the f -mode frequencies of the initial NSs for nearly equal-mass binaries. Our work potentially brings GW asteroseismology to the late-inspiral and merger phases of BNS systems, filling the gap between the early inspiral and post-merger signals.

ACKNOWLEDGEMENTS

The authors thank Alan Tsz-Lok Lam and Chun-Lung Chan for useful discussions and comments on the manuscript. This work was partially supported by grants from the Research Grants Council of the Hong Kong (Project No. CUHK 24304317 and CUHK 14306419), the Croucher Innovation Award from the Croucher Foundation Hong Kong, and by the Direct Grant for Research from the Research Committee of the Chinese University of Hong Kong.

[1] Kent Yagi, Koutarou Kyutoku, George Pappas, Nicolás Yunes, and Theodoros A Apostolatos. Effective no-hair

relations for neutron stars and quark stars: relativistic results. *Physical Review D*, 89(12):124013, 2014.

- [2] Ignacio F Ranea-Sandoval, Octavio M Guilera, Mauro Mariani, and Milva G Orsaria. Oscillation modes of hybrid stars within the relativistic cowling approximation. *Journal of Cosmology and Astroparticle Physics*, 2018(12):031, 2018.
- [3] C Vásquez Flores, Alessandro Parisi, Chian-Shu Chen, and Germán Lugones. Fundamental oscillation modes of self-interacting bosonic dark stars. *Journal of Cosmology and Astroparticle Physics*, 2019(06):051, 2019.
- [4] Leor Barack, Vitor Cardoso, Samaya Nissanke, Thomas P Sotiriou, Abbas Askar, Chris Belczynski, Gianfranco Bertone, Edi Bon, Diego Blas, Richard Brito, et al. Black holes, gravitational waves and fundamental physics: a roadmap. *Classical and quantum gravity*, 36(14):143001, 2019.
- [5] Nikolaos Stergioulas, Andreas Bauswein, Kimon Zagkouris, and Hans-Thomas Janka. Gravitational waves and non-axisymmetric oscillation modes in mergers of compact object binaries. *Monthly Notices of the Royal Astronomical Society*, 418(1):427–436, 2011.
- [6] Geraint Pratten, Patricia Schmidt, and Tanja Hinderer. Gravitational-wave asteroseismology with fundamental modes from compact binary inspirals. *Nature communications*, 11(1):1–7, 2020.
- [7] Thierry Mora and Clifford M Will. Post-newtonian diagnostic of quasidequilibrium binary configurations of compact objects. *Physical Review D*, 69(10):104021, 2004.
- [8] Éanna É Flanagan and Tanja Hinderer. Constraining neutron-star tidal love numbers with gravitational-wave detectors. *Physical Review D*, 77(2):021502, 2008.
- [9] Jocelyn S Read, Luca Baiotti, Jolien DE Creighton, John L Friedman, Bruno Giacomazzo, Koutarou Kyutoku, Charalampos Markakis, Luciano Rezzolla, Masaru Shibata, and Keisuke Taniguchi. Matter effects on binary neutron star waveforms. *Physical review D*, 88(4):044042, 2013.
- [10] Tuhin Malik, N Alam, M Fortin, C Providência, BK Agrawal, TK Jha, Bharat Kumar, and SK Patra. Gw170817: Constraining the nuclear matter equation of state from the neutron star tidal deformability. *Physical Review C*, 98(3):035804, 2018.
- [11] Benjamin P Abbott, Richard Abbott, TD Abbott, F Acernese, K Ackley, C Adams, T Adams, P Addesso, Rana X Adhikari, Vaishali B Adya, et al. Gw170817: Measurements of neutron star radii and equation of state. *Physical review letters*, 121(16):161101, 2018.
- [12] I Tews, J Margueron, and S Reddy. Critical examination of constraints on the equation of state of dense matter obtained from gw170817. *Physical Review C*, 98(4):045804, 2018.
- [13] Wynn CG Ho. Gravitational waves from neutron stars and asteroseismology. *Philosophical Transactions of the Royal Society A: Mathematical, Physical and Engineering Sciences*, 376(2120):20170285, 2018.
- [14] Patricia Schmidt and Tanja Hinderer. Frequency domain model of f-mode dynamic tides in gravitational waveforms from compact binary inspirals. *Physical Review D*, 100(2):021501, 2019.
- [15] Tanja Hinderer, Andrea Taracchini, Francois Foucart, Alessandra Buonanno, Jan Steinhoff, Matthew Duez, Lawrence E Kidder, Harald P Pfeiffer, Mark A Scheel, Bela Szilagyi, et al. Effects of neutron-star dynamic tides on gravitational waveforms within the effective-one-body approach. *Physical review letters*, 116(18):181101, 2016.
- [16] Jan Steinhoff, Tanja Hinderer, Alessandra Buonanno, and Andrea Taracchini. Dynamical tides in general relativity: effective action and effective-one-body hamiltonian. *Physical Review D*, 94(10):104028, 2016.
- [17] Nils Andersson and Kostas D Kokkotas. Towards gravitational wave asteroseismology. *Monthly Notices of the Royal Astronomical Society*, 299(4):1059–1068, 1998.
- [18] Harald Dimmelmeier, Nikolaos Stergioulas, and José A Font. Non-linear axisymmetric pulsations of rotating relativistic stars in the conformal flatness approximation. *Monthly Notices of the Royal Astronomical Society*, 368(4):1609–1630, 2006.
- [19] A Bauswein and H-T Janka. Measuring neutron-star properties via gravitational waves from neutron-star mergers. *Physical review letters*, 108(1):011101, 2012.
- [20] Kentaro Takami, Luciano Rezzolla, and Luca Baiotti. Constraining the equation of state of neutron stars from binary mergers. *Physical Review Letters*, 113(9):091104, 2014.
- [21] Luciano Rezzolla and Kentaro Takami. Gravitational-wave signal from binary neutron stars: a systematic analysis of the spectral properties. *Physical Review D*, 93(12):124051, 2016.
- [22] Andreas Bauswein, Nikolaos Stergioulas, and Hans-Thomas Janka. Exploring properties of high-density matter through remnants of neutron-star mergers. *The European Physical Journal A*, 52(3), Mar 2016.
- [23] Junaid Aasi, BP Abbott, Richard Abbott, Thomas Abbott, MR Abernathy, Kendall Ackley, Carl Adams, Thomas Adams, Paolo Addesso, RX Adhikari, et al. Advanced ligo. *Classical and quantum gravity*, 32(7):074001, 2015.
- [24] F Acernese, M Agathos, K Agatsuma, D Aisa, N Allemandou, A Allocca, J Amarni, P Astone, G Balestri, G Ballardin, et al. Advanced virgo: a second-generation interferometric gravitational wave detector. *Classical and Quantum Gravity*, 32(2):024001, 2014.
- [25] Yoichi Aso, Yuta Michimura, Kentaro Somiya, Masaki Ando, Osamu Miyakawa, Takanori Sekiguchi, Daisuke Tatsumi, Hiroaki Yamamoto, KAGRA Collaboration, et al. Interferometer design of the kagra gravitational wave detector. *Physical Review D*, 88(4):043007, 2013.
- [26] M Punturo, M Abernathy, F Acernese, B Allen, Nils Andersson, K Arun, F Barone, B Barr, M Barsuglia, M Beker, et al. The einstein telescope: a third-generation gravitational wave observatory. *Classical and Quantum Gravity*, 27(19):194002, 2010.
- [27] Kentaro Takami, Luciano Rezzolla, and Luca Baiotti. Spectral properties of the post-merger gravitational-wave signal from binary neutron stars. *Physical Review D*, 91(6):064001, 2015.
- [28] Tim Dietrich, Sebastiano Bernuzzi, Maximiliano Ujevic, and Wolfgang Tichy. Gravitational waves and mass ejecta from binary neutron star mergers: Effect of the stars’ rotation. *Physical Review D*, 95(4):044045, 2017.
- [29] Tim Dietrich, Maximiliano Ujevic, Wolfgang Tichy, Sebastiano Bernuzzi, and Bernd Brügmann. Gravitational waves and mass ejecta from binary neutron star mergers: Effect of the mass ratio. *Physical Review D*, 95(2):024029, 2017.
- [30] Patrick Chi-Kit Cheong, Lap-Ming Lin, and Tjonnie Guang-Feng Li. Gmunu: Toward multigrid based einstein field equations solver for general-relativistic hydro-

- dynamics simulations. *Classical and Quantum Gravity*, 2020.
- [31] Jocelyn S Read, Benjamin D Lackey, Benjamin J Owen, and John L Friedman. Constraints on a phenomenologically parametrized neutron-star equation of state. *Physical Review D*, 79(12):124032, 2009.
- [32] Sebastiano Bernuzzi, Alessandro Nagar, Simone Balmelli, Tim Dietrich, and Maximiliano Ujevic. Quasiuniversal properties of neutron star mergers. *Physical Review Letters*, 112(20):201101, 2014.
- [33] TK Chan, Y-H Sham, PT Leung, and L-M Lin. Multipolar universal relations between f-mode frequency and tidal deformability of compact stars. *Physical Review D*, 90(12):124023, 2014.
- [34] N Bucciantini and L Del Zanna. General relativistic magnetohydrodynamics in axisymmetric dynamical spacetimes: the x-echo code. *Astronomy & Astrophysics*, 528:A101, 2011.
- [35] AG Pili, N Bucciantini, and L Del Zanna. Axisymmetric equilibrium models for magnetized neutron stars in general relativity under the conformally flat condition. *Monthly Notices of the Royal Astronomical Society*, 439(4):3541–3563, 2014.
- [36] A Akmal, VR Pandharipande, and DG Ravenhall. Equation of state of nucleon matter and neutron star structure. *Physical Review C*, 58(3):1804, 1998.
- [37] F Douchin and P Haensel. A unified equation of state of dense matter and neutron star structure. *Astronomy & Astrophysics*, 380(1):151–167, 2001.
- [38] L Engvik, G Bao, M Hjorth-Jensen, E Osnes, and E Osetaard. Asymmetric nuclear matter and neutron star properties. *arXiv preprint nucl-th/9509016*, 1995.
- [39] Mark Alford, Matt Braby, Mark Paris, and Sanjay Reddy. Hybrid stars that masquerade as neutron stars. *The Astrophysical Journal*, 629(2):969, 2005.
- [40] Norman K Glendenning. Neutron stars are giant hypernuclei? 1984.
- [41] NK Glendenning and SA Moszkowski. Reconciliation of neutron-star masses and binding of the λ in hypernuclei. *Physical review letters*, 67(18):2414, 1991.
- [42] John Antoniadis, Paulo CC Freire, Norbert Wex, Thomas M Tauris, Ryan S Lynch, Marten H van Kerkwijk, Michael Kramer, Cees Bassa, Vik S Dhillon, Thomas Driebe, et al. A massive pulsar in a compact relativistic binary. *Science*, 340(6131), 2013.
- [43] Amiram Harten, Peter D Lax, and Bram van Leer. On upstream differencing and godunov-type schemes for hyperbolic conservation laws. *SIAM review*, 25(1):35–61, 1983.
- [44] Dmitri Kuzmin and Stefan Turek. High-resolution fctvd schemes based on a fully multidimensional flux limiter. *Journal of Computational Physics*, 198(1):131–158, 2004.
- [45] Motoyuki Saijo. The collapse of differentially rotating supermassive stars: conformally flat simulations. *The Astrophysical Journal*, 615(2):866, 2004.
- [46] Isabel Cordero-Carrión, Pablo Cerdá-Durán, Harald Dimmelmeier, José Luis Jaramillo, Jérôme Novak, and Eric Gourgoulhon. Improved constrained scheme for the einstein equations: An approach to the uniqueness issue. *Physical Review D*, 79(2):024017, 2009.
- [47] A Bauswein, H-T Janka, K Hebeler, and A Schwenk. Equation-of-state dependence of the gravitational-wave signal from the ring-down phase of neutron-star mergers. *Physical Review D*, 86(6):063001, 2012.
- [48] A Bauswein, N Stergioulas, and H-T Janka. Revealing the high-density equation of state through binary neutron star mergers. *Physical Review D*, 90(2):023002, 2014.
- [49] Thibault Damour and Alessandro Nagar. Effective one body description of tidal effects in inspiralling compact binaries. *Physical Review D*, 81(8):084016, 2010.
- [50] James M Lattimer and F Douglas Swesty. A generalized equation of state for hot, dense matter. *Nuclear Physics A*, 535(2):331–376, 1991.
- [51] Luca Baiotti, Bruno Giacomazzo, and Luciano Rezzolla. Accurate evolutions of inspiralling neutron-star binaries: Prompt and delayed collapse to a black hole. *Physical Review D*, 78(8):084033, 2008.
- [52] Thibault Damour, Alessandro Nagar, and Loic Villain. Measurability of the tidal polarizability of neutron stars in late-inspiral gravitational-wave signals. *Physical Review D*, 85(12):123007, 2012.
- [53] Nils Andersson and Pantelis Pnigouras. The seismology of love: An effective model for the neutron star tidal deformability. *arXiv preprint arXiv:1905.00012*, 2019.
- [54] CG Ho Wynn and Lai Dong. Resonant tidal excitations of rotating neutron stars in coalescing binaries. *Monthly Notices of the Royal Astronomical Society*, 308(1):153–166, 1999.
- [55] Sizheng Ma, Hang Yu, and Yanbei Chen. Excitation of f-modes during mergers of spinning binary neutron star. *Physical Review D*, 101(12), Jun 2020.
- [56] Huan Yang. Inspiralling eccentric binary neutron stars: Orbital motion and tidal resonance. *Phys. Rev. D*, 100:064023, Sep 2019.
- [57] Michelle Vick and Dong Lai. Tidal effects in eccentric coalescing neutron star binaries. *Phys. Rev. D*, 100:063001, Sep 2019.
- [58] Dong Lai. Resonant oscillations and tidal heating in coalescing binary neutron stars. *Monthly Notices of the Royal Astronomical Society*, 270(3):611–629, 1994.
- [59] Masaru Shibata. Effects of tidal resonances in coalescing compact binary systems. *Progress of Theoretical Physics*, 91(5):871–883, 1994.
- [60] Eanna E Flanagan and Etienne Racine. Gravitomagnetic resonant excitation of rossby modes in coalescing neutron star binaries. *Physical Review D*, 75(4):044001, 2007.
- [61] Roman Gold, Sebastiano Bernuzzi, Marcus Thierfelder, Bernd Brügmann, and Frans Pretorius. Eccentric binary neutron star mergers. *Physical Review D*, 86(12):121501, 2012.